JOURNAL OF GEOPHYSICAL RESEARCH, VOL. 96, NO. A1, PAGES 87-99, JANUARY 1, 1991

A LARGE-AMPLITUDE ROTATIONAL WAVE IN THE VENUSIAN IONOSHEATH

A.O. Fedorov and O.L. Vaisberg

Space Research Institute, Moscow, USSR

D. S. Intriligator

Carmel Research Center, Santa Monica, California

R.Z. Sagdeev[1] and A.A. Galeev

Space Research Institute, Moscow, USSR

Abstract. We report the results of a preliminary analysis of a large-amplitude rotational wave in the Venusian ionosheath. Our results are based on an analysis of the Pioneer Venus Orbiter plasma and magnetic field observations from six orbits in the first (1979) tail season. This wave appears to be the standing superalfvenic wing. It is located within the shocked plasma flow outside the boundary of the tail. The rotation of the magnetic field by about 90 deg across the wave occurs through several successive cycles making the wave similar to the group velocity wing consisting of phase velocity waves. The transition through the wave is accompanied by the vector change of the plasma velocity with the magnitude of the plasma velocity jump comparable to the vector jump of the Alfven velocity. The observed super-Alfvenic wing appears to originate upstream and closer to the planet, possibly near the upper boundary of the magnetic barrier on the dayside.

Introduction

Observations of the Venusian environment performed on a number of space probes showed the existence of a bow shock and a distinct tail (see, for example, the review of Russell and Vaisberg, 1983). The first plasma measurements made by Bridge et al. (1967), on Mariner 5 showed the existence of a rarified and decelerated ion flux within the shocked solar wind flow (usually called the ionosheath or magnetosheath) around Venus. This region, adjacent to the Venusian tail, also was observed in ion measurements on the Venera 9 and Venera 10 orbiters as the region with varying and modified ion spectra - the boundary layer (Vaisberg et al. 1976). This region occupies a significant part of the ionosheath (Figure 1). The second ion component in the lower energy range of ionosheath spectra suggested that ion pickup was occurring in this region.

Russell (1976) made an analysis of the first magnetic field measurements performed on Venera 4 and Mariner 5 and showed the existence of the current layer well above the boundary of the Venusian tail. Its location (see Figure 1) suggests that it could be associated with the boundary layer.

Perez-de-Tejada et al. (1984, 1985) examined the Pioneer Venus Orbiter (PVO) plasma and electric field observations and found evidence of varying and modified ion and angular spectra and of local plasma turbulent processes that may also be indicative of a boundary layer. Analyses of the PVO data also provided evidence of ion pick-up: observations of a high-energy peak in the ion spectra, in this case with energy about 16 times the energy of the shocked solar wind protons. This suggested the acceleration of planetary oxygen ions (Mihalov et al., 1980; Intriligator, 1982).

In the present paper we consider simultaneous plasma and magnetic field measurements obtained on Pioneer Venus Orbiter (PVO) within the Venusian ionosheath at distances 11-12 radii of Venus, R_V, downstream of the planet.

PVO was inserted in an elliptical orbit around Venus in December 1978, with a period of revolution of approximately 24 hours and an inclination to the equator of 105° (Colin, 1980). With the apogee height 66,900 km and with the low-latitude location of periapsis (17°N), PVO crosses the Venusian tail at distances from about 8 to 12 R_V. Because of the orbital motion of Venus around the Sun this happens about every 225 days. This period of time that includes about 10 tail crossings is called the tail season.

For analysis in this paper we selected six orbits (orbits 181, 183, 185, 186, 187, and 188) from the first PVO tail season. We do not consider the tail itself. The purpose of this paper is to analyze the properties of the current layer previously noticed by Russell (1976) that perhaps corresponds to the boundary of the boundary layer. We will analyze the magnetic field data for two orbits in more detail and will show that this current layer leads to the rotation of the magnetic field vector by about 90° without significantly changing its magnitude. We will then show that the vector change of the magnetic field is accompanied by the change of the plasma velocity vector. These changes will be compared to the conditions for the rotational discontinuity.

We will also speculate on the connection of the analyzed current layer with the current forming the Venusian tail.

[1]Now at Physics Department, University of Maryland, College Park.

Copyright 1991 by the American Geophysical Union

Paper number 90JA01841.
0148-0227/91/90JA-01841$05.00

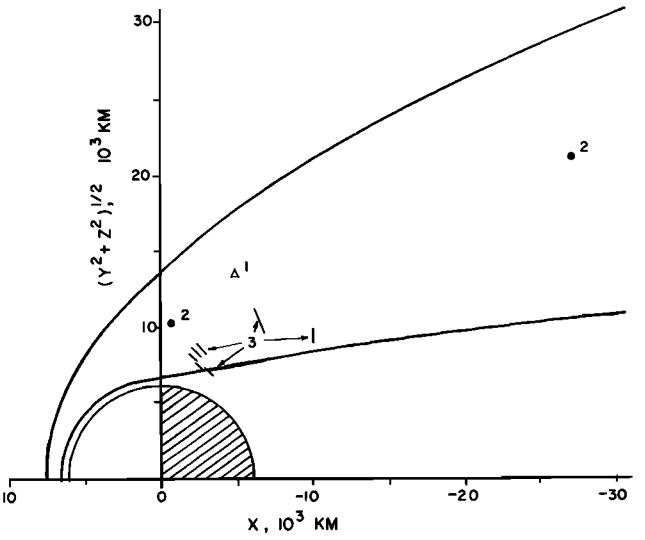

Fig. 1. Boundaries in the near-Venusian space as observed in early experiments. Current layer crossings identified in Venera 4 (1), Mariner 5 (2), magnetic field data by Russell (1976), and the boundary layer's boundary according to Venera 9 and Venera 10 plasma measurements (Vaisberg et al., 1976).

Instrumentation

The plasma analyzer (Intriligator et al., 1980) consists of quadrispheric electrostatic analyzer followed by five collectors. Its field of view is fan shaped and has an angular width of 15° in the plane perpendicular to the spacecraft axis of rotation and an angular width of 140° in the plane of the spacecraft rotation axis. This 140° total angular coverage is divided into five collectors with three center collectors each having an angular width of 15° and two outer collectors each having an angular width of 47°. The Pioneer Venus Orbiter spin rate is approximately 5 RPM around an axis approximately perpendicular to the ecliptic plane (Colin, 1980). The 360° azimuthal direction is divided into 512 sectors. Thus the plasma analyzer views most of the sphere, and its central window views the belt of 15° centered around the ecliptic plane.

The plasma analyzer was in the high-energy ion scan mode during the time intervals studied in this paper. In this mode the energy per unit charge (E/Q) range from 50 to 8000 eV is covered in 32 logarithmically spaced energy steps. The instrument scans on one energy step per spacecraft rotation and transmits the maximum ion flux and the direction of the azimuthal and polar angles associated with this maximum flux. A new 32 step set of measurements begins every 9 min. This is followed by polar and azimuthal scans at the four E/Q steps about the peak flux of the scan.

The magnetometer (Snare and Means, 1977) is a three-axis fluxgate magnetometer providing vector measurements with sampling rate of 1/s. We have used 12-second averages kindly provided by C. T. Russell.

Observations

The sequences of ion energy spectra measured along the preapoapsis portion of two PVO orbits: orbit 188 (day 161, 1979) and orbit 185 (day 158, 1979) are shown in Figure 2a and 2b, respectively. The trajectories corresponding to this portion of these orbits are shown in Figure 2c and 2d in Venus-centered solar-orbital coordinates with the X axis directed toward the Sun, and the Y axis directed opposite to the direction of Venus orbital motion and the Z axis completing the orthogonal system. $R_{YZ} = (Y^2+Z^2)^{\frac{1}{2}}$ is the distance from the X axis. The average location of tail is indicated (Russell and Vaisberg, 1983, Saunders and Russell, 1986).

We will discuss orbit 188 first because the ionosheath was more quiet during this pass and presumably as a result all regions and boundaries are more distinct on this pass. In the beginning of the time interval shown (first five spectra in Figure 2a) we see the steady ionosheath flow far downstream from the planet. The ion spectra have two components: one with higher intensity, occupying the lower energy part of the spectrum, and a smaller one at higher energies. Their relative location on the E/Q scale (the energy ratio is about 2) and relative ion flux show that they are, respectively, the proton and alpha components of solar-wind-origin plasma moving with approximately equal speeds. Their distinct separation on the E/Q spectrum, similar to what usually observed in the solar wind, is the result of plasma acceleration and cooling of the plasma, heated on the bow shock, well downstream of the obstacle to the solar wind flow.

In the time interval starting at about 0850 UT, when the spacecraft approaches the tail, we see significant fluctuations of the speed of ion flow without noticeable changes in the shape of the ion spectrum. More significant changes start at about 1030 UT: deceleration of the flow, widening of the spectrum, less distinct separation of the two ion components. These features characterize the boundary layer (Bridge, et al., 1967; Vaisberg et al. 1976).

At about 1140 UT the ion flux drops drastically. Most of the spectra observed afterward show very small fluxes of low-energy ions. The change of plasma regime with the disappearance of the shocked solar wind plasma and the transition to the region where low-energy ions or no ion flux was observed was considered by Vaisberg et al., (1976), as an indication of crossing of the tail boundary, and we identify the time interval starting at about 1140 UT as the tail. Some of the spectra observed in the tail and near the tail boundary have two components: lower energy similar to that reported by Vaisberg et al. (1976) and interpreted as the mantle ions of planetary origin, and higher-energy ions as discussed by Mihalov et al. (1980) and by Mihalov and Barnes (1981, 1982) and by Intriligator (1982, 1989), in terms of the pick-up of planetary oxygen ions.

Many similar features are observed on orbit 185 (Figure 2b). The first five spectra in the time interval shown indicate a slightly disturbed ionosheath. At about 0800 UT the spacecraft entered the region of speed fluctuations. Stronger modifications of the ion spectra start

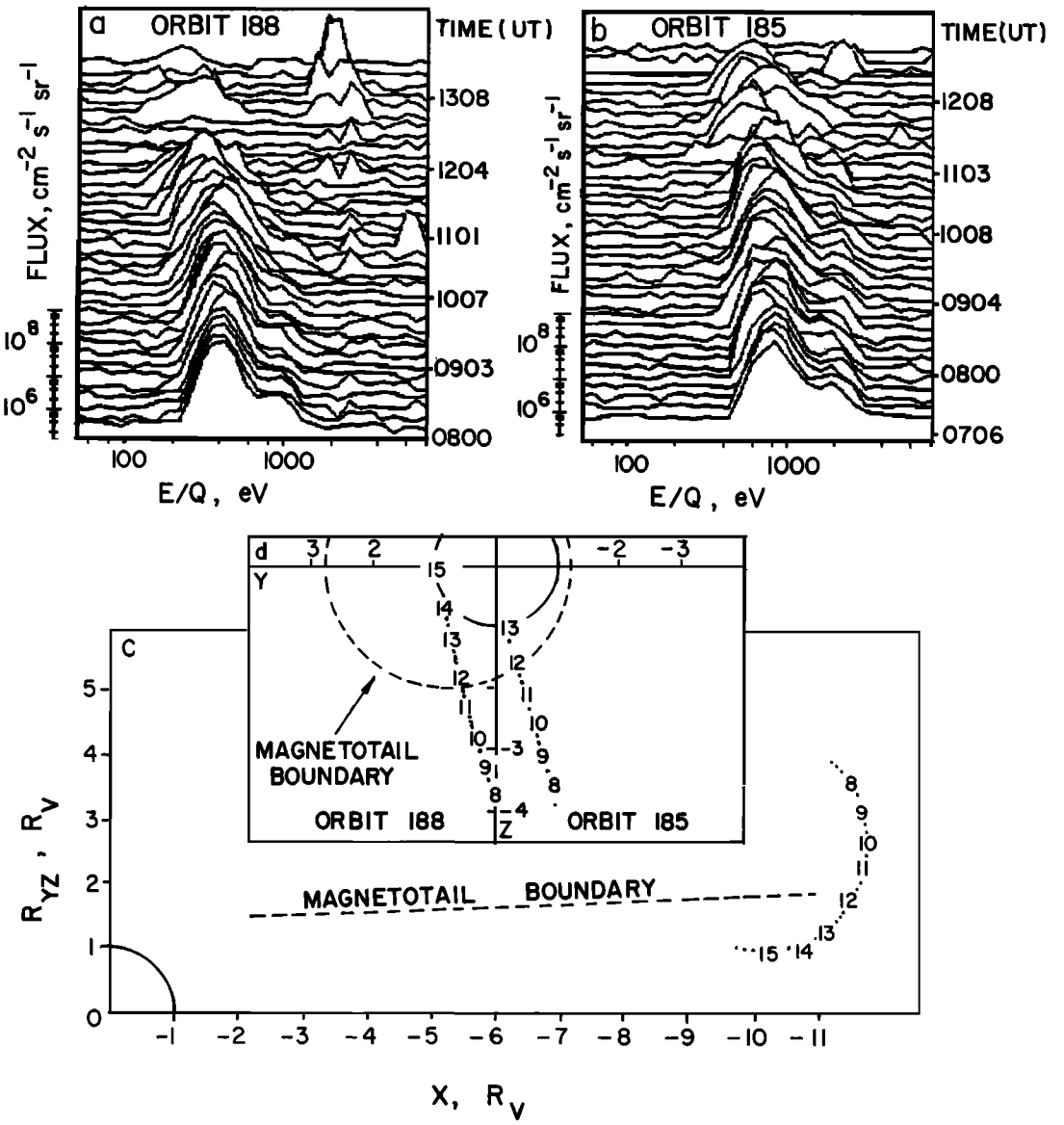

Fig. 2. (a)Succession of the ion spectra observed on the preapoapsis part of PVO orbit 188. The shape of the variability of ion spectra define different regions of near-Venus space: relatively steady flow in the ionosheath (first five spectra), disturbed spectra of the boundary layer, and low or unobservable flux in the tail. Higher-energy ions appear near the tail boundary. The spacecraft approached the tail moving from the -Z direction to the tail axis from 4.5 to 1.5 R_v at the distance of -11 R_v to -12 R_v downstream of the planet. (b) The same for orbit 1985. (c) and (d) Parts of PVO orbits in Venus-centered coordinate system (two projections). The average location of the tail boundary is indicated.

at about 0950 UT. The deceleration of ions across the boundary layer is less clearly seen as compared with orbit 188. The spacecraft first enters the tail at about 1045 UT as shown by the change of ion population (unobservable or very small fluxes of low-energy ions). The subsequent series of ion spectra (time interval 1110-1205 UT) may be associated with reentering the boundary layer although the spectra differ in shape and energy from those observed before the tail crossing.

The plasma and magnetic field data from the preapoapsis parts of orbits 188 and 185 are shown together in Figure 3. The upper part of each plot is a modification of the more conventional plot of the energy-time spectrogram of ions. All measurements are shown by bars at every E/Q step with the length of the bar proportional to the logarithm of the ion flux. The origin of each bar is located at the point in the energy-time spectrogram, where the specific measurement was made. The energy-time plane is simultaneously

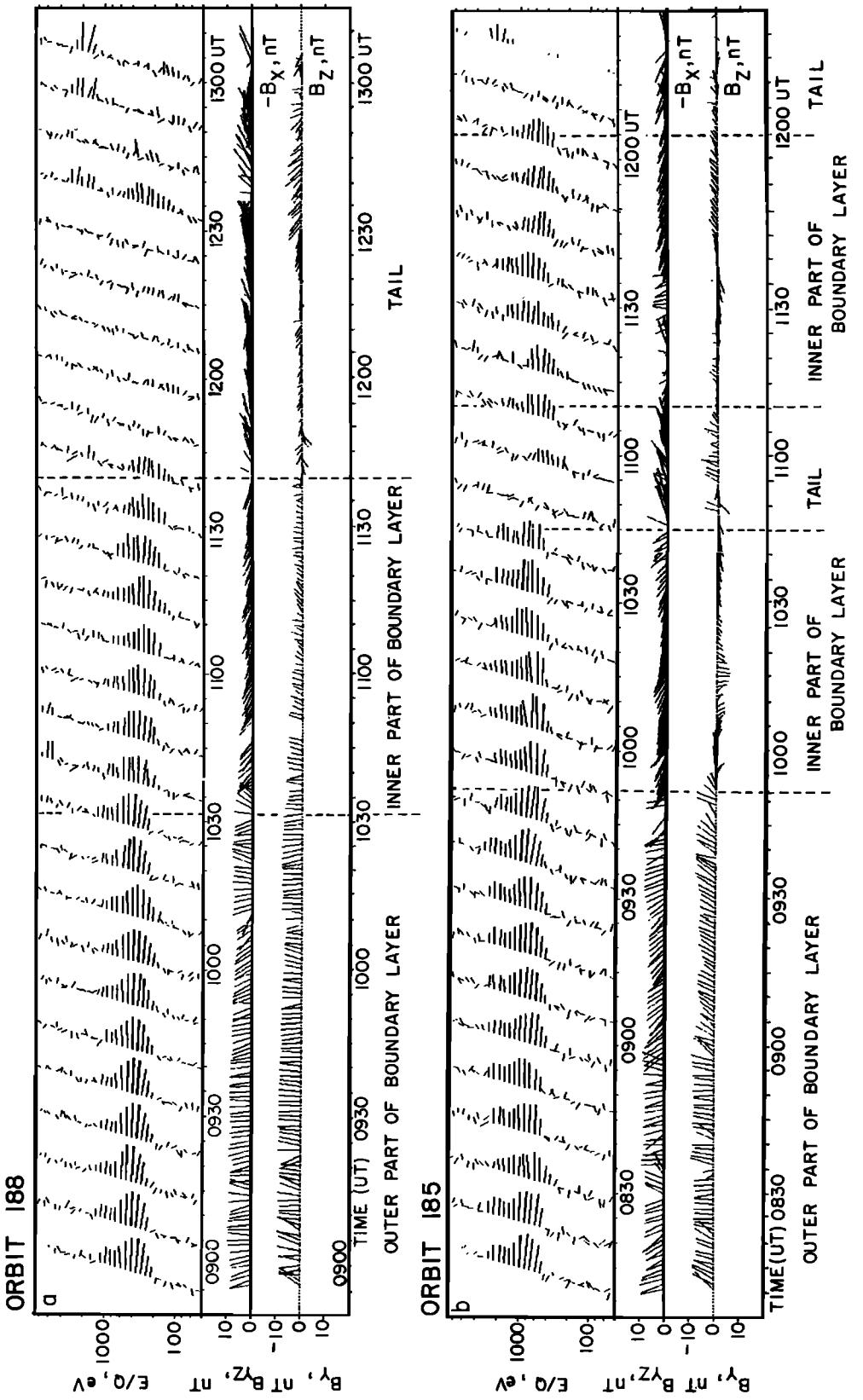

Fig. 3. (a) Simultaneous plasma and magnetic field measurements on the preapoapsis part of orbit 188. The upper panel shows the energy-time spectrogram of ions together with the direction of maximum flux at each energy step. The two lower panels show the magnetic field observations. Various plasma and magnetic regimes are indicated (see text). (b) The same for the preapoapsis part of orbit 185.

superposed on the orbital plane in order to indicate flow direction. The Sun-directed X axis is aligned with the time axis, where +X is opposite to the direction of increasing time and with the Y axis (lying in the orbital plane and directed opposite to the direction of orbital motion of Venus) aligned with the energy axis with +Y values corresponding to decreases in energy. The Sun is to the left relative to the part of the plane shown. The direction of each bar corresponds to the azimuthal direction of the maximum flux (at the specific E/Q step) as measured by the plasma spectrometer. The aberrated solar wind would be represented in this coordinate system by an arrow deflected (from the horizontal direction) to the bottom of the frame. In the very low-energy and high-energy ranges the instrumental noise is dominating, as indicated by the random directions of arrows. An average level of this noise corresponds to a flux level of about 5×10^5 $cm^{-2}s^{-1}$ per energy step.

The two lower panels of each plot show the magnetic field along the orbit. The 12-s averages are shown as the vectors along the time scale with their origins indicating the start time of the measurements. Every fifth of the magnetic field vectors are shown in order to avoid overlapping. The middle panel shows the transverse magnetic field $B_{yz} = \sqrt{B_y^2+B_z^2}$ versus B_x component with $+B_x$ to the left. The bottom panel shows the B_y component versus B_z component (in this case the +Z axis, which is perpendicular (north) to the orbital plane, which is coaligned with the time scale, is to the right).

Figure 3a shows the plasma and magnetic field data for part of orbit 188 including the boundary layer and part of the tail. As discussed above, we have identified different plasma regimes. The plot shows that in the outer part of the boundary layer the ion spectra have two components: protons and alphas of the solar-wind-origin plasma moving with approximately equal speeds. Another interesting feature of the spectra is that the direction of the maximum flux is changing with energy. This is more clearly seen in the proton component. This indicates that the proton distribution function is significantly anisotropic.

This pass shows relatively small perturbations of the magnetic field in the outer part of the boundary layer (after about 1032 UT more significant fluctuations are seen in the ion spectra and the magnetic field orientation changes). The direction of the magnetic field in this region is quite close to that observed in the undisturbed ionosheath outside the boundary layer. A change of orientation of the magnetic field resulting in an increase of the B_x component corresponds to the magnetic field line draping which is associated with mass loading (Alfven, 1957). The spacecraft enters the tail at about 1140 UT, as determined by low or unobservable fluxes of ions (or by higher-energy ions as discussed by Intriligator, 1982, 1989). Further discussion of the tail is outside the scope of this paper, and the reader is referred to relevant publications. We note that the direction of the magnetic field in the inner part of the boundary layer (from about 1035 to 1140 UT) is opposite to the direction observed within the Venus tail.

Figure 3b shows the plasma and magnetic field data for part of orbit 185 including the boundary layer and part of the tail. The magnetic field data show that the magnetic field in the outer part of the boundary layer is more disturbed compared with that in orbit 188. The magnitude of the magnetic field is not strongly changing, but the direction of the field is almost continually varying. As we can see these variations are mainly associated with the changes in the orientation of the B vector relative to the X axis. The direction of the magnetic field that was observed within the time intervals centered at 0850 and 0935 UT is close to the undisturbed magnetic field which was persistent in the ionosheath before the time interval shown.

Again, we see intervals when the B_x component increases, corresponding to magnetic field line draping in connection with mass loading. In the majority of these cases the B_x component increases in the +X direction, and the ion energy spectra retain, as a rule, an ionosheathlike appearance. In some cases B_x turns in the -X direction, and in the longest time interval, from 1047 to 1106 UT, this was accompanied by a drop in ion flux below the sensitivity level of the instrument or by the appearance of low-energy ions indicating the spacecraft was in the tail region. An alternative approach to identifying the tail was employed by Dolginov et al. (1978) and by Saunders and Russell (1986) whose analyses were based on the magnitude and orientation of the magnetic field. Our experience with the plasma and magnetic field measurements near Venus suggests that the more reliable identification of the tail requires the consideration of the simultaneous plasma and magnetic field measurements (Vaisberg et al., 1976; Intriligator and Scarf, 1984). At the same time it appears quite natural to consider as a tail or a wake everything that is inside the external (shocked solar wind) flow. We will not elaborate on this topic anymore as this paper is on another subject. On the basis of the above arguments we consider the time interval 1047-1106 UT as the tail. In the subsequent time interval the spacecraft was intermittently in the ionosheath and in the tail.

It can be seen in Figure 3 that when the magnetic disturbances are long enough the temporal resolution of the plasma spectrometer allows one to find the accompanying disturbances in the ion spectra in the ionosheath. These disturbances are seen as the fluctuations in the shape of the ion spectra and in the flow directions. There is also a deceleration of the flow in orbit 185 at 0835 and after about 0855 UT. These are the features of the near-tail boundary layer plasma observed on Venera 9 and 10 (Vaisberg et al., 1976). It is worth while to note once again that in the boundary layer plasma the changes in the B_x component are, in most cases, in a different direction than the direction of the magnetic field in the tail (time intervals 1047-1106 UT and after 1205 UT for orbit 185).

Data Analysis

In order to more clearly identify the different regimes in the region downstream of Venus we performed a cluster analysis of the magnetic field components. The scatterplots of the magnetic field components should reveal distinct configurations of the magnetic field.

The results of the cluster analysis for the B_x and B_y magnetic field components for the time interval 0900-1210 UT on orbit 188 are shown in Figure 4a to 4c. The different time intervals corresponding to the various plasma regimes are shown separately to more clearly demonstrate the clustering of the magnetic field in the different regions of near-Venus space. The time interval 0900-1000 UT (Figure 4a) corresponds to the perturbations in the outer part of the boundary layer and is characterized by relatively small deflections of the magnetic vector from the nearly -Y aligned direction (as in the ionosheath) to the +X direction. The B vector rotates mainly in the XY plane and simultaneously displays rotations in the YZ plane (not shown). There are smaller changes in orientation in the XY plane.

Figure 4b (time interval 1000-1100 UT) approximately corresponds to the transition from the outer to the inner part of the boundary layer and is characterized by large-scale variations of the magnetic field. During the time interval the magnetic field vector rotates by about 90°. At the end of this time interval the magnetic field becomes predominantly X aligned.

The transition from the inner part of the boundary layer to the Venusian tail (time interval 1110-1210 UT) is shown in Figure 4c. It is characterized by a change of sign in the B_x component.

Figure 4d to 4f show the results of the cluster analysis of the magnetic field for the selected time intervals of orbit 185. The different regions are also clearly separated in this case, the outer part of the boundary layer with significant fluctuations (Figure 4d, 0900-0940 UT), the transition from the outer to the inner part of the boundary layer (Figure 4e, 0930-1020 UT), and the transition from the boundary layer to the tail (Figure 4f). As in the previous case, the magnetic field rotates by about 90° at the transition from the ionosheath to the boundary layer and by about 180° at the tail boundary.

We performed a minimum variance analysis of the magnetic field near the transition from the outer part of the boundary layer to its inner part. We employed the conventional procedure described by Sonnerup and Cahill (1967). The results of the minimum variance analysis of the magnetic field measurements from orbit 188 during the time interval of the transition (1012-1042 UT) are shown in Figure 5a. The observed

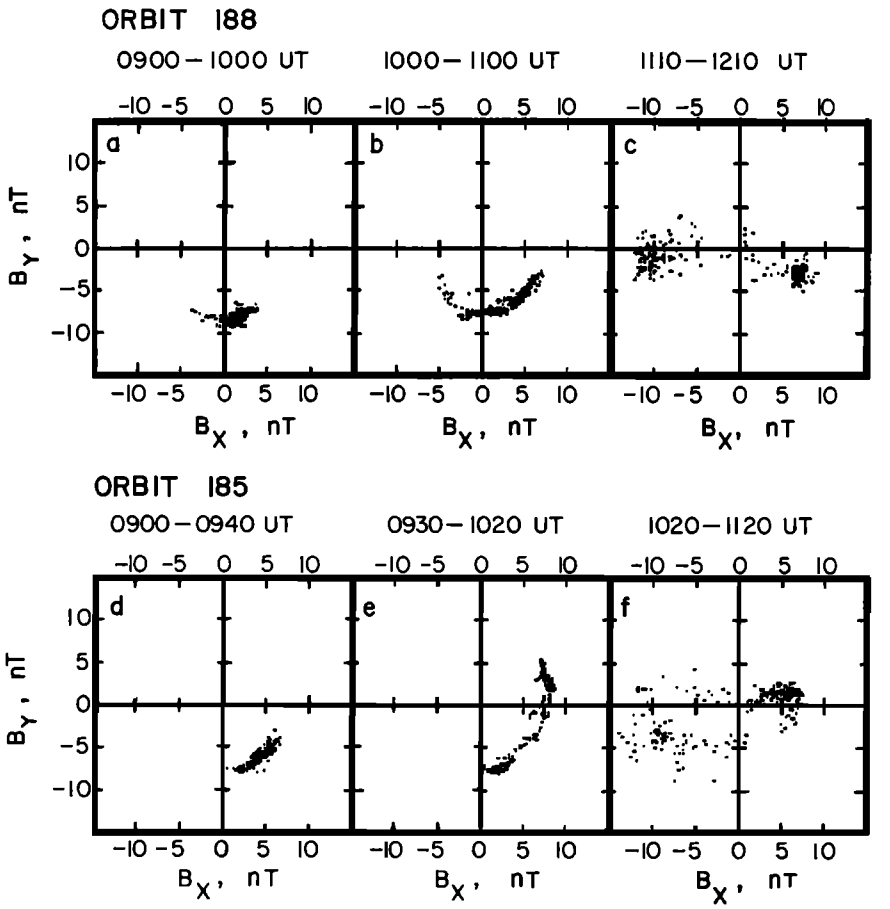

Fig. 4. Cluster analysis of the magnetic field components (a), (b), and (c) orbit 188 and (d), (e), and (f) orbit 185:
Figure 4a and 4d - for the outer part of the boundary layer;
Figure 4b and 4e - for the transition from the outer part of the boundary layer to the inner part of it;
Figure 4c and 4f - for the transition from the boundary layer to the tail.

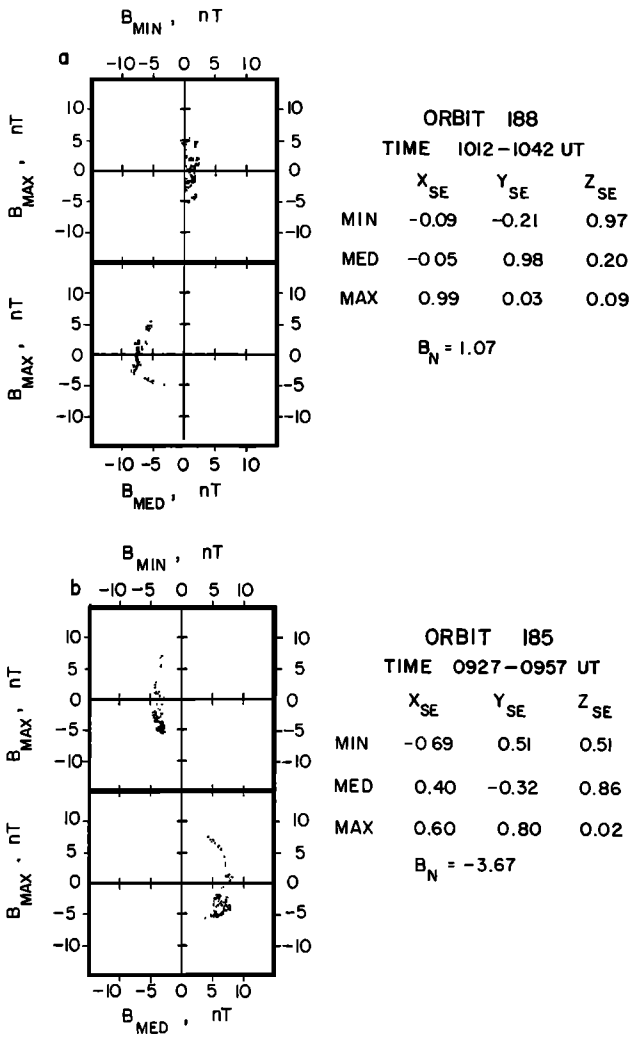

Fig. 5. Minimum variance analysis of the magnetic field disturbances at the transition from the outer part of the boundary layer to the inner part of it observed on (a) orbit 188 and on (b) orbit 185. Two projections are shown for each orbit: B_{max} versus B_{min} (upper) and B_{max} versus B_{med} (lower).

variation corresponds to a rotational wave with strong overlapping variations and with a normal component of 1.53 nT. The direction of minimum variances (i.e., the normal direction) in the solar-orbital coordinate system is (-0.09, -0.21,0.97). The definitely smaller scatter of the data along the minimum variance axis as compared with the other axes shows the significance of the obtained result. This gives an angle of ≈ 75° between the normal to the wave and the direction of the magnetic field in the less disturbed region in the external part of the boundary layer, just prior to the crossing of the wave.

Figure 5b shows the results of a minimum variance analysis of the magnetic field observed on orbit 185 during the time interval corresponding to the transition from the outer part of the boundary layer to the inner part of it (0927-0957 UT). This transition is also a rotational wave overlapped by large-amplitude fluctuations in the magnetic field. In this case the analysis shows a strong normal component (≈ 3.7 nT). The direction of the minimum variance is (-0.69,0.51, 0.51). Again, the smaller scatter of the points along the calculated minimum variance direction suggests the result is meaningful. The angle between the direction of minimum variance to this packet and the magnetic field in the less disturbed part of the external boundary layer, just outside the wave, is about 129°.

Figure 6 shows the profiles of the magnetic field components and the magnitude in the "normal" coordinate system with the N axis directed along the calculated minimum variance direction of the large amplitude wave; the M axis is directed perpendicular to both the N axis and to the X' axis that is directed along the average aberration angle of the solar wind, 5° (the positive direction of M is determined by the vector product N×X'); and the L axis completes the orthogonal system. The magnetic field profiles for two orbits allow us to identify several regions. Region 1 is the ionosheath outside the boundary layer. It is much more quiet for orbit 188 than for orbit 185. Region 2 separates the two different magnetic field regions - the ionosheath, including the external part of the boundary layer, and the internal part of the boundary layer. Within this part of the flow around the tail, namely, the internal part of the boundary layer the magnetic field direction is strikingly different from the direction of the magnetic field in the tail (region 3). It seems remarkable that the large-amplitude rotational waves (regions 2) have quite a similar appearance in the two cases.

A more detailed examination of the behavior of the L component of the magnetic field in region 2 shows that:

1. In the beginning of this region the field starts to turn toward the X direction, namely, the direction of the field in the magnetic tail (see 1013 to 1023 UT in orbit 188 and 0930 to 0943 UT in orbit 185).
2. The rotational wave itself (see 1023 to 1040 UT in orbit 188 and 0943 to 0957 UT in orbit 185) leads to the change in direction of the magnetic field to the direction nearly antiparallel to the Venus tail magnetic field direction.
3. The change in the magnetic field within the wave occurs in a nonmonotonic manner as if the spacecraft crossed the peaks and troughs of phase standing waves.

The time scale of the event in the frame of reference of the spacecraft is not long enough to trace the change in the ion distribution function across the structure of the wave. However, it is possible to do so by grouping together the ion measurements made at various E/Q steps in association with the various orientations of the magnetic field.

An attempt to reveal the correspondence of the ion distribution function variations to the magnetic field changes across the wave for orbit 188 is shown in Figure 7a for the time interval 0930-1130 UT which includes the crossing of the rotational wave. Only the proton E/Q range was considered. Each ion measurement performed in the high energy scan mode described above is represented by a circle in the equatorial plane

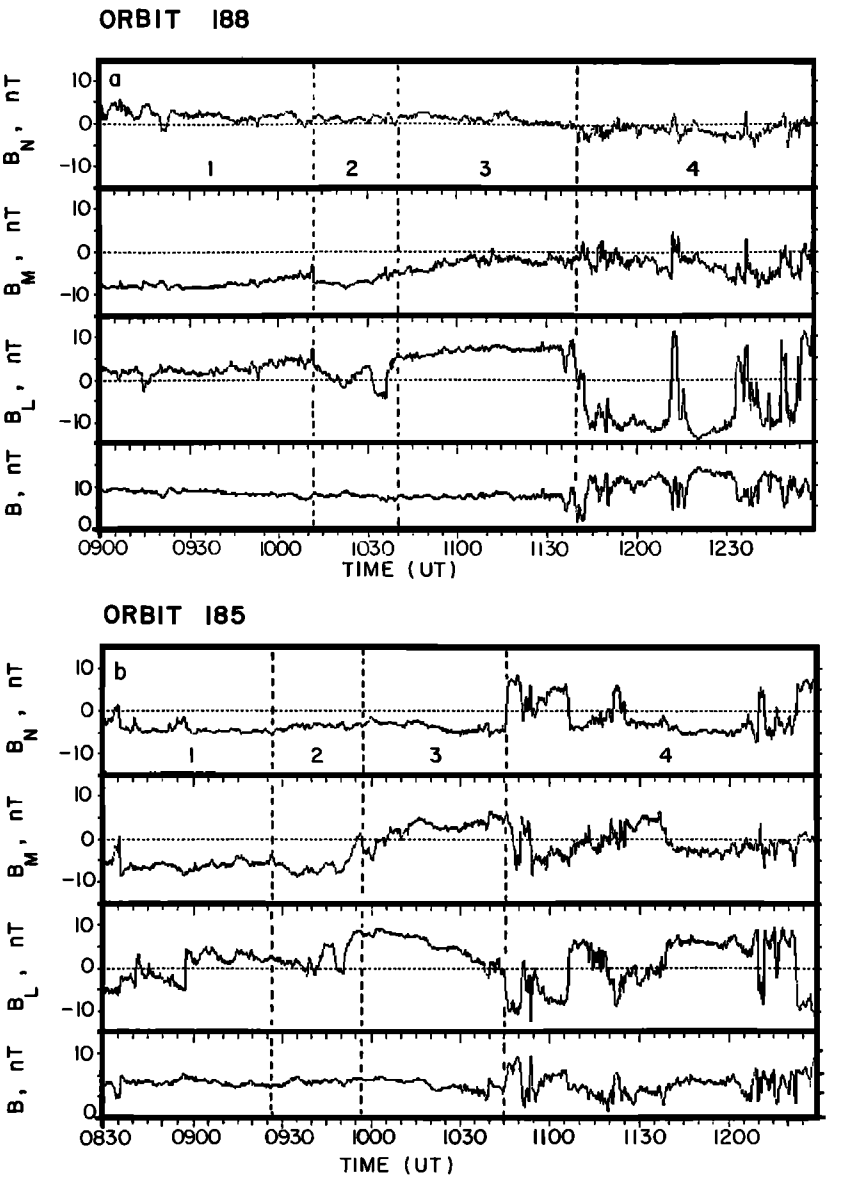

Fig. 6. The components of the magnetic field in the N, M, L coordinate system (see text) and the magnetic field magnitude for parts of orbits (a) 188 and (b) 185. Different regions are indicated: (1) ionosheath and/or the outer part of the boundary layer, (2) rotational wave, (3) inner part of the boundary layer, and (4) the tail.

of velocity space (with coordinates V_x, V_y). The diameter of the circle is proportional to the logarithm of the ion density in phase space. The minimum counting rate considered as meaningful was chosen as 1.6 of the average noise level of the instrument. The arrow drawn from the center of each circle shows the equatorial components (B_x, B_y) of the magnetic field that were measured simultaneously with the ion observations.

It is evident that the direction of the azimuthal flow associated with the maximum flux at each E/Q step is systematically changing with the change in the orientation of the magnetic field. The total change in orientation of B was $\approx 80°$. It also can be seen that the proton distribution function is not isotropic (an isotropic distribution function of the convected flow would have directions of maximum flux at all energies located along the straight line passing through the origin of the coordinate system). During an E/Q scan (i.e., not a polar scan) the precision of the measurement of the ion velocity component in the polar direction is significantly less than that for the azimuthal component. Since the changes in the B_x and B_y components through the wave are larger than the change in the B_z component, and since the measurements of the changes in the total energy of the ions and flow direction show that the main variations of flow velocity are in the XY plane, comparison of the variations of the flow direction in XY plane with the variations of the magnetic field in the same plane is representative.

Figure 7b shows the result of a parametric

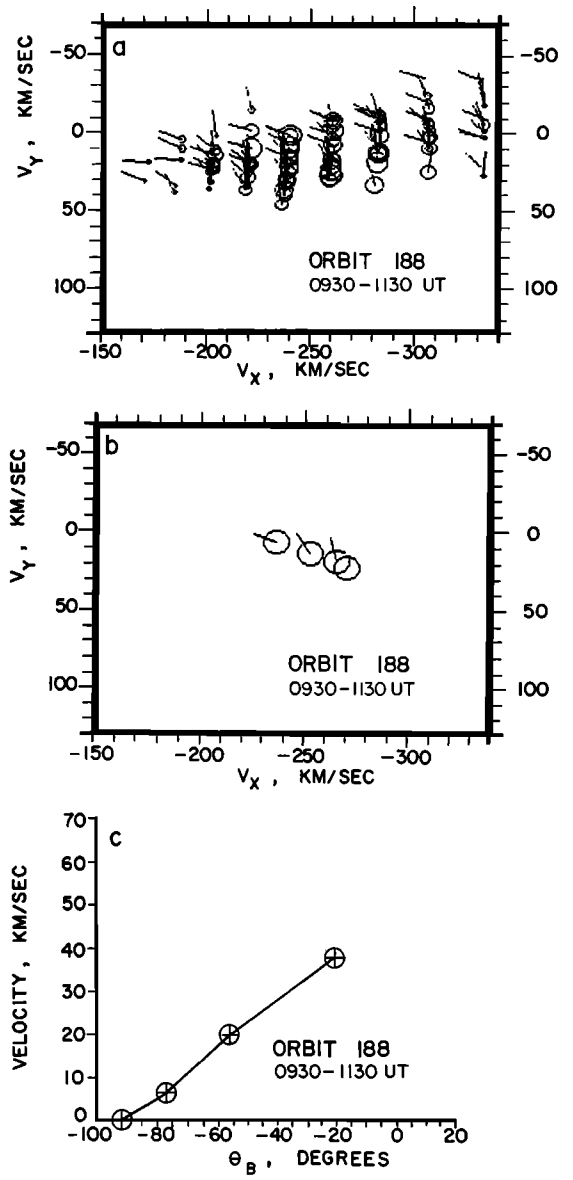

Fig. 7. (a)The locations of ion counts maxima at specific energy steps on the V_x, V_y plane of velocity space as measured in the time interval 0930-1130 UT on (a) orbit 188. The diameter of the circle drawn at each point of velocity space is proportional to the logarithm of the ion phase space density. Simultaneous measured magnetic field components in the XY plane are shown as vectors, originating at the center of their respective circles. (b) The variation of the magnitude of proton velocity vector component in the V_x, V_y plane across the rotational wave determined from ion spectra selected according to specific angular sectors of magnetic field orientation. The arrow drawn from the center of each circle is the magnetic field vector obtained from the magnetic field measurements within each sector weighted by the number of plasma measurements with nonzero counting rate. The time sequence corresponds to anticlockwise motion of the circle starting from higher absolute value of V. (c) The magnitude of the vector velocity variation versus the direction of the magnetic field vector in the XY plane (θ_B). The time sequence is from left to right.

study of the proton distribution function. Namely, the data for the proton component were separated as a function of the measured orientation of the magnetic field in the XY plane. The azimuthal angle is the angle measured from the +X direction counterclockwise. The azimuthal angular interval between ≈ -90° and ≈ -10° through which the magnetic vector rotates was divided into four sectors in such a way so that there are a significant number of ion measurements with nonzero flux within each sector. All measurements of the proton flux for each of these four magnetic sectors were grouped together to form a synthesized proton spectrum. The vector velocity in the XY plane was calculated in each of these sectors:

$$\bar{V} = \frac{\Sigma n_i \bar{V}_i}{\Sigma n_i} \qquad (1)$$

where n_i is the phase space density in the point $\bar{V}_i$ of the velocity space. The magnetic field data for each sector were weighted by the number of plasma measurements with nonzero counting rate. From Figure 7b we can see that the proton vector velocity changes systematically as a function of the change in the orientation of the magnetic field. This systematic change of the magnitude and direction of the vector velocity with the orientations of magnetic field vector is shown quantitatively on Figure 7c. The magnitude of the vector velocity change across the wave was ≈ 37 km/s. The accuracy in this figure is about 2 km/s.

Figure 8 is similar to Figure 7 and gives the result of the analysis of velocities and magnetic field orientation for orbit 185. The total variation of the vector velocity across the wave was ≈ 63 km/s. The magnetic field vector rotates by ≈ 97°. Again, the plasma velocity changes systematically with the change of orientation of the magnetic field.

Figure 9 shows the six orbits in the PVO first tail season that we have considered. The coordinate system used is the V × B system with the axes determined as follows: the X′ axis is directed along the average aberration angle of the solar wind, i.e., 5° west of the Sun, the Y′ axis lies in the plane containing the X′ axis and the B_{yz} (transverse to the B_x component of the interplanetary magnetic field) component of IMF in the positive direction of this component, and the Z′ axis completes the orthogonal system. Different orbits can cross each other in this coordinate system.

Three of the orbits (183, 185, and 188) show clear evidence of a rotational wave. The magnetic field component traces on two of the other orbits, 181 and 187, and, with lesser certainty, on the remaining orbit 186, indicate the presence of a rotational wave. The disadvantage of these six orbits, however, is that all of them lie in the same sector in the V,B coordinate system. Additional orbits should be considered to determine the properties of the boundary layer and of the rotational wave as a function of various sectors of the V,B coordinate system and as a function of other parameters (for example, the sign of B_x).

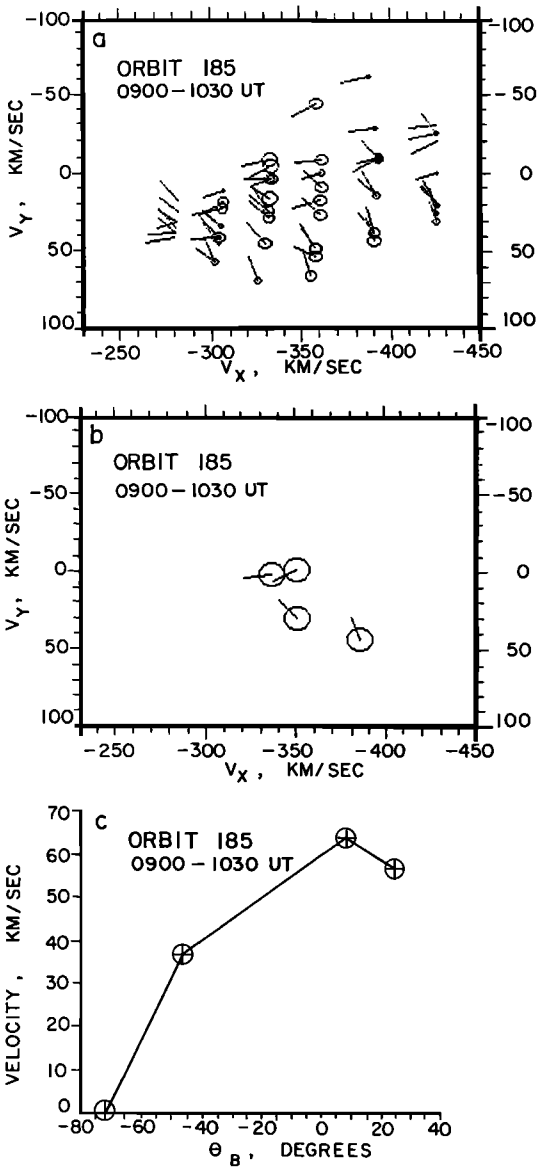

Fig. 8. The same for the rotational wave observed on orbit 185. Time sequence corresponds to anticlockwise motion of the circle starting from the higher absolute value of V(b) and is from left to right in (c).

Discussion

The rotational wave considered in this paper appears to be a stationary feature that exists in the ionosheath outside the tail boundary. The location of the standing rotational Alfven wave we report at Venus suggests that it originates somewhere upstream of the place of observation. It is quite probable that it is the continuation of the boundary reported earlier as a current layer (Russell, 1976) and as a boundary of the boundary layer (Vaisberg et al. 1976; Perez-de-Tejada et al., 1984, 1985). In this case the source region of current that drives the wave may lie somewhere on the dayside or at the terminator, possibly near the upper boundary or within the magnetic barrier (Elphic et al. 1980). A similar boundary appears to exist in the shocked solar wind flow around Mars (Vaisberg, 1976; Intriligator and Smith, 1979).

The Alfven signature of a conducting body moving through a magnetized plasma was previously reported at Io (Ness et al., 1979). Subsequently, it was shown to be the sub-Alfvenic wing drawn by current through the ionosphere or through Io itself induced by the motion of Io in the Jovian magnetic field (Neubauer, 1980; Goertz, 1980; Southwood et al., 1980). This Alfven wing is limited to the magnetic field tube with a diameter not significantly larger than Io itself. The most significant difference in the Venusian case compared with that at Io is that the Venusian standing wave is in super-Alfvenic flow, while Io's wing is in sub-Alfvenic flow. It appears also from analysis of Io's wing that the current flows in one direction from one side of Io and in the opposite direction from the other side of Io. The observed rotation in the direction of the magnetic field that we find across the wave is opposite to the direction of the magnetic field in the Venusian tail and

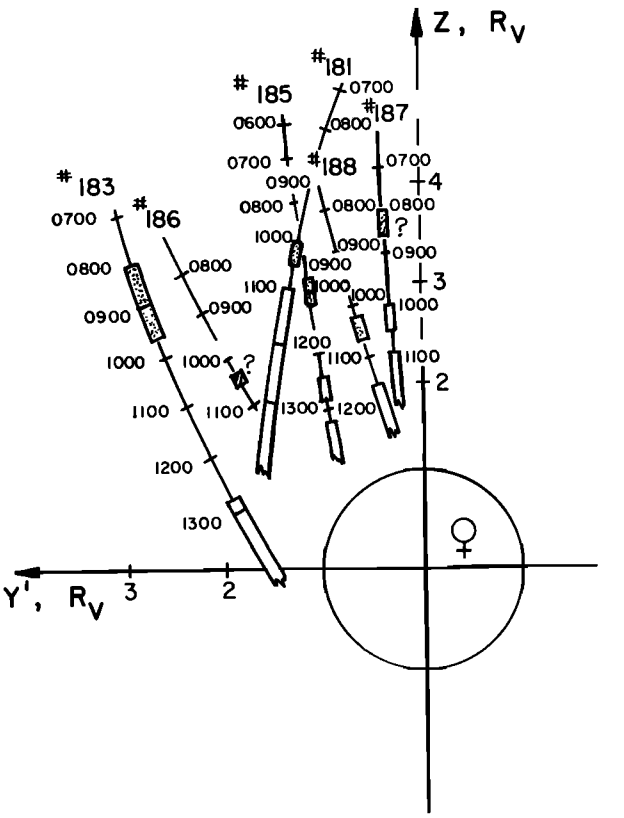

Fig. 9. The coverage of the distant ionosheath by 6 PVO orbits from the first tail season in the rotated reference frame determined by the orientation of the magnetic field in the ionosheath. The orbits are displayed in a V, B coordinate system where the X' axis is directed +5°W of the Sun in the Venus orbital plane, the Y' axis is in the plane containing the perpendicular component of the magnetic field in the ionosheath outside of the boundary layer. The time (hours, UT) is indicated along each orbit. The locations of the rotational wave are shown by black segments. The white segments along each orbit indicate where the spacecraft crossed the tail.

suggests that at Venus the current flowing along the boundary of the tail may partly close through the current flowing in the Alfven wave (see Figure 6). If this is the case, then the magnetic field in the boundary layer may be an important part of all the magnetic structure developing near the gaseous obstacle. It would be interesting to investigate the relationship of the Alfven wave to the magnetic barrier and to the magnetic tail, but this would demand the analysis of a significantly larger amount of data. We hope to do this in the future. Vaisberg and Zeleny (1984) argued that the magnetic barrier is topologically connected to the Venusian tail. If this is the case, the Alfven wave could be triggered by currents associated with the pickup of ions as was suggested for Io (Goertz, 1980). At Venus this may occur in the region above or within the magnetic barrier. This is consistent with the increased levels of turbulence at Venus that are associated with ion pickup (Intriligator and Scarf, 1982).

Conditions to be fulfilled for the rotational discontinuity are

$$V_n = B_n \cdot (4\pi\rho)^{-1/2}$$
$$(\underset{-}{V}_t) = (\underset{-}{B}_t) \cdot (4\pi\rho)^{-1/2} \qquad (2)$$

(Landau and Lifshitz, 1960) where $\rho = m \cdot N$ is the density of the plasma, m and N are, respectively, the mass and the number density of ions, n and t correspond to the normal and to the transverse to the normal directions, and the brackets denote the difference of the vector values on the two sides of the discontinuity. The difficulty in performing the comparison between the theory and the observations lies in the fact that the spacecraft is moving transversely to the lines of the plasma flow. As a result of the significant thickness of the transition (that lies in the range of a few thousand kilometers) the upstream and downstream plasma parameters are measured within the different flow lines. Additional error may be caused by the uncertainty in V_z but this does not appear to be significant (see below).

The plasma and magnetic field parameters used for comparison of the measurements with the conditions for a rotational discontinuity (equation 2) are shown in Table 1. In order to calculate (vector) jump conditions we selected two time intervals before (time interval 1) and after (time interval 2) the wave crossing on the two orbits. These time intervals, corresponding to the time frame of the plasma measurements, were chosen as close as possible to the rotational wave itself. Plasma parameters (V_x,V_y,N,T) were calculated with the use of a Maxwellian fit to the proton part of the ion spectra. Comparison of the velocity values calculated with the Maxwellian fit and with the help of the moments calculations show that the accuracy of the velocity value usually lies within $\pm$ 2 km/s. Calculating the N we have taken into account that the angular aperture of the instrument is comparable with the angular width of the ion flow. This gives an additional error to the calculated number density in spite of the fact that the calibration of the instrument is well known. We calculate that the number densities are correct within a factor of $\pm$ 20%.

The computed plasma parameters show nearly continuous changes across the waves on the two orbits. The proton number densities are average values across the discontinuities. The jumps of the Alfven velocities were calculated with the mass and the calculated number densities of protons. The jumps of proton velocities were calculated assuming that $V_{z1} = V_{z2} = 0$. Allowance for the V_z jump will increase the value of the $(V_{t2}-V_{t1})$ by about several percent for both cases as we can judge from the comparison of the B_z jumps with the jumps of the two other magnetic field components. There are several uncertainties that may lead to the errors in obtained values and to the deviation of calculated jumps from the conditions (equation 2). They may be due to (1) the previously mentioned displacement of the spacecraft transverse to the plasma flow lines while crossing the wave since the measured velocity jump is not the same as that observed along the flow line; (2) the deviation of the proton distribution function from a Maxwellian; (3) no allowance for the alpha particle and heavy ion contributions to the plasma density that will slightly decrease the computed Alfven velocity. With this in mind we can conclude with some degree of confidence that the observe rotational wave satisfies the conditions for a rotational discontinuity (equation 2).

TABLE 1. Plasma and Magnetic Field Parameters

Orbit No.	188		185	
Region	Upstream (1)	Downstream (2)	Upstream (1)	Downstream (2)
Time Interval, UT	1016-1025	1043-1052	0932-0941	1009-1031
B_x,B_y,B_z, nT	-1.1,-7.8,-0.9	4.9, -5.1, 1.1	2.3,-7.4,3.6	7.5, 4.0, 0.4
V_x,V_y, km/s	-274, 22	-250, 13	-381, 48	-341, -9
N, cm^{-3}		24		18
$(B_2-B_1)\cdot(3\pi\rho)^{-1/2}$, km/s		31		66
$(V_{t2}-V_{t1})$,* km/s		25		70

*Assuming $V_{z1} = V_{z2} = 0$.

The existence of the Alfven signature at Io and at Venus shows that it could be a universal feature of the interaction of moving magnetized plasmas with a broad range of obstacles. This suggests that the mystery boundary observed near Comet Halley midway between the shock and the comet itself (Reme et al., 1986) also may be the Alfven signature. Perez-de-Tejada (1989) also has noted the possible relation of the mystery boundary to the boundary layer at Venus.

Acknowledgments. Two of the authors (A. O. Fedorov and O. L. Vaisberg) are thankful to Carmel Research Center for the opportunity to visit and to work at the Center for three months in 1988. This work was supported by the Pioneer Venus Project Office under NAS2-12313 and NAS2-12912, by Carmel Research Center, and by Space Research Institute (IKI).

The Editor thanks J. L. Phillips and another referee for their assistance in evaluating this paper.

References

Alfven, H., On the theory of comet tails, Tellus, 9, 92-96, 1957.

Bridge, H. S., A. J. Lazarus, C. W. Snyder, E. J. Smith, P. J. Coleman, and D. E. Jones, Plasma and magnetic field near Venus, Science, 158, 1669-1673, 1967.

Colin, L., The Pioneer Venus program, J. Geophys. Res., 85, 7575-7589, 1980.

Dolginov, Sh. Sh., L. N. Zhuzgov, V. A. Sharova, and B. V. Buzin, Magnetic field and magnetosphere of the planet Venus, Kosm. Issled., 16, 837-863, 1978.

Elphic, R. C., C. T. Russell, J. A. Slavin, L. M. Brace, The location of the dayside ionopause of Venus: Pioneer Venus orbiter magnetometer observations, Geophys. Res. Lett., 7, 561-564, 1980.

Goertz, C. K., Io's interaction with plasma torus, J. Geophys Res., 85, 2949-2956, 1980.

Intriligator, D. S., Observations of mass addition to the shocked solar wind of the Venusian ionosheath, Geophys. Res. Lett., 9, 727-730, 1982.

Intriligator, D. S., Results of the first statistical study of Pioneer Venus orbiter plasma observations in the distant Venus tail: Evidence for a hemispheric asymmetry in the pickup of ionospheric ions, Geophys. Res. Lett., 16, 167-170, 1989.

Intriligator, D. S., and F. L. Scarf, Plasma turbulence in the downstream ionosheath of Venus, Geophys. Res. Lett., 9, 1325-1328, 1982.

Intriligator, D. S., and E. J. Smith, Mars in the solar wind, J. Geophys. Res., 84, 8427-8435, 1979.

Intriligator, D. S., J. H. Wolfe, and J. D. Mihalov, The Pioneer Venus orbiter plasma analyzer experiment, IEEE Trans. Geosci. Remote Sens., GE-19, 39, 1980.

Landau, L. D., and E. I. Lifshitz, in Electrodynamics of Continuous Media, Addison-Wesley, Reading Mass., 1960.

Mihalov, D. D., and A. Barnes, Evidence for the acceleration of ionospheric O^+ in the magnetosheath of Venus, Geophys. Res. Lett., 8, 1277-1280, 1981.

Mihalov, J. D., and A. Barnes, The distant interplanetary wake of Venus: Plasma observations from Pioneer Venus, J. Geophys. Res., 87, 9045-9053, 1982.

Mihalov, J. D., J. H. Wolfe, D. S. Intriligator, Pioneer Venus plasma observations of the solar-wind-Venus interaction, J. Geophys. Res., 85, 7613-7624, 1980.

Ness, N. F., M. N. Acuna, R. P. Lepping, L. F. Burlaga, K. W. Behannon, and F. N. Neubauer, Magnetic field studies at Jupiter by Voyager 1: Preliminary results, Science, 204, 982-987, 1979.

Neubauer, F. M., Nonlinear standing Alfven wave current system at Io: Theory, J. Geophys. Res., 85, 7, 1171-1178, 1980.

Perez-de-Tejada, H., Viscous flow interpretation of Comet Halley's mystery transition, J. Geophys. Res., 94, 10,131-10,136, 1989.

Perez-de-Tejada, H., D. S. Intriligator, and F. L. Scarf, Plasma and electric field measurements of the PVO in the Venus ionosheath, Geophys. Res. Lett., 11, 31-34, 1984.

Perez-de-Tejada, H., D. S. Intriligator, and F. L. Scarf, Plasma measurements of the Pioneer Venus orbiter in the Venus ionosheath: Evidence for plasma heating near the ionopause, J. Geophys. Res., 90, 1759-1764, 1985.

Reme, H., J. A. Sauvaud, C. d'Uston, A. Cros, K. A. Anderson, C. W. Carlson, D. W. Cortis, R. P. Lin, A. Korth, A. K. Richter and D. A. Mendis, General features of the comet Halley - Solar wind interaction, Exploration of Halley Comet, Vol. 1, edited by B. Battrick, E. J. Rolfe, and R. Reinhard, Eur. Space Agency Spec. Publ., 250, pp. 29-34, 1986.

Russell, C. T., The magnetopause of Venus: Evidence for a boundary layer and a magnetotail, Geophys. Res. Lett., 3(10), 589-592, 1976.

Russell, C. T., and O. L. Vaisberg, The interaction of the solar wind with Venus, in Venus, edited by D. M. Hunten, L. Colin, T. M. Donahue, and V. I. Moroz, pp. 873-940, University of Arizona Press, Tucson, 1983.

Saunders, M. A., and C. T. Russell, Average dimension and magnetic structure of the distant Venus magnetotail, J. Geophys. Res., 91, 5589-5604, 1986.

Southwood, D. J., M. G. Kivelson, R. J. Walker, and J. A. Slavin, Io and its plasma environment, J. Geophys. Res., 85, 5959-5968, 1980.

Snare, R. C., and J. D. Means, Pioneer Venus orbiter fluxgate magnetometer, IEEE Trans. Magn., MAG-13, 1107-1109, 1977.

Sonnerup, B. U. O., and L. J. Cahill, Jr., Magnetopause structure and attitude from Explorer 12 observations, J. Geophys. Res., 72, 171-183, 1967.

Vaisberg, O. L., Mars-plasma environment, in Physics of Solar Planetary Environment, edited by D. J. Williams, pp. 854-871, AGU, Washington, D.C., 1976.

Vaisberg, O. L., and L. M. Zeleny, Formation of plasma mantle in the Venusian magnetosphere, Icarus, 58, 412-430, 1984.

Vaisberg, O. L., S. A. Romanov, V. N. Smirnov, I. P. Karpinsky, B. I. Khazanov, B. V. Polenov,

A. V. Bogdanov, and N. M. Antonov, Ion flux parameters in the solar wind-Venus interaction region according to Venera 9 and Venera 10 data, in Physics of Solar Planetary Environment, edited by D. J. Williams, pp. 904-917, AGU, Washington, D.C., 1976.

A. O. Fedorov, A. A. Galeev, and O. L. Vaisberg, Space Research Institute, Profsoyuznaya 84/32, Moscow 117810, USSR.

D. S. Intriligator, Camel Research Center, Post Office Box 1732, Santa Monica, CA 90406.

R. Z. Sagdeev, Physics Department, University of Maryland, College Park, MD 20742.

(Received September 6, 1988;
revised July 12, 1990;
accepted July 12, 1990.)